

Electron Spin-Lattice Relaxation in Phosphorus-Doped Silicon*

A. HONIG AND E. STUPP†

Syracuse University, Syracuse, New York

(Received July 23, 1959)

Electron spin-lattice relaxation in phosphorus-doped silicon has been investigated over a magnetic field range of 0 to 11 000 oersteds, a temperature range of 1.25°K to 4.2°K, and a concentration range of 10^{14} P/cc to 3×10^{16} P/cc. Three distinct $\tau_S(\Delta m_S = \pm 1, \Delta m_I = 0)$ relaxation mechanisms have been identified, and their functional dependences on magnetic field, temperature, and concentration have been determined. These mechanisms are characterized as follows: (a) $(1/\tau_S)(H^4, T)$ is concentration independent, and has an H^4 and T dependence. At 3000 oersteds and 1.25°K, $(1/\tau_S)(H^4, T) = (2.63 \pm 0.10) \times 10^{-5} \text{ sec}^{-1}$. (b) $(1/\tau_S)(T^7)$ is independent of concentration and magnetic field, and has a T^7 dependence. At 2.00°K, $1/\tau_S(T^7) = (1.65 \pm 0.15) \times 10^{-4} \text{ sec}^{-1}$. (c) $(1/\tau_S)(\text{conc.})$ depends linearly on concentration for concentrations below 10^{16} P/cc, and has approximately an H^{-1} and T dependence. At 3000 oersteds and 1.25°K, $1/\tau_S(\text{conc.})$ for a 4×10^{16} P/cc sample is $3.3 \pm 0.4 \times 10^{-4} \text{ sec}^{-1}$. In addition to these three τ_S mechanisms, the horizontal relaxation modes ($\Delta m_I = \pm 1, \Delta m_S = 0, \pm 1, \mp 1$) were investigated. $1/\tau_X(\Delta m_I = \pm 1, \Delta m_S = \mp 1)$ at 2.16°K is independent of concentration and magnetic field, and between 2.16°K and 4.2°K, has a $T^{0.5}$ temperature dependence; all of which strongly suggests a dominant Raman process in this temperature region. At 2.16°K, $\tau_X = 3.0 \pm 0.4$

hours. At 1.25°K, the magnetic field dependence of the horizontal modes was measured. The large errors (associated with the very long times involved) make it difficult to ascertain the dominant mechanism here. However, our results are not consistent with a quadratic magnetic field dependence of $1/\tau_X$. At low magnetic fields, concentration dependent $\tau_N(\Delta m_I = \pm 1, \Delta m_S = 0)$ and τ_X mechanisms arise, due to an admixture of states which allows $1/\tau_S(\text{conc.})$ also to induce $1/\tau_N$ and $1/\tau_X$ transitions. When all the preceding mechanisms are properly superposed, their resultant agrees well with the experimental relaxation probabilities, except for a small discrepancy which shows up for dilute samples at 1.25°K. This discrepancy ($\sim 2 \times 10^{-5} \text{ sec}^{-1}$ at 1.25°K) can be accounted for by introducing another mechanism. There is some indication that this mechanism is associated with the amount of compensation.

The theoretical origins of the mechanisms are discussed. A theory is proposed to explain the concentration dependent τ_S mechanism, according to which rapidly relaxing close pairs of phosphorus atoms, which are few in number, relax the spins of the large number of isolated phosphorus atoms via a spin diffusion process. Experiments supporting this hypothesis are presented.

I. INTRODUCTION

THE spins of the paramagnetic electrons associated with phosphorus impurities in silicon¹ can relax from a nonequilibrium distribution by many mechanisms. In this paper, the various spin-lattice relaxation mechanisms are separated out, the properties of each of the mechanisms are determined, and the theoretical origins of the mechanisms are discussed. The results shed light on the general magnetic moment-phonon interaction problem, and elucidate some important properties of the silicon host crystal as well.

The experiments consist mostly of measurements of the electron spin-lattice relaxation times at various magnetic fields and temperatures.² From an experimental point of view, impurity-doped silicon lends itself to a thorough study of electron paramagnetic relaxation at low temperatures (liquid helium) because of the very long relaxation times encountered. This feature enables one to measure magnetic field dependence over a very large range of magnetic fields with a single frequency paramagnetic resonance equipment. As it turns out, X-band (about 9000 megacycles/sec) is very suitable and has been used

throughout this study. The magnetic field range we have investigated is from 0 to 11 000 oersteds, and the temperature range is from 1.2°K to 4.2°K. Phosphorus concentrations ranged from 10^{14} P/cc to 3×10^{16} P/cc. Minority impurity concentration (compensation) was also varied. The choice of phosphorus as the donor impurity eliminates the possibility of nuclear quadrupole relaxation effects, since the nuclear spin of phosphorus is $\frac{1}{2}$.

Modes of spin relaxation involving solely spin-spin (no phonon) interactions, and those involving electron exchange between bound and conduction electrons are not treated in this paper, but are reserved for two subsequent reports dealing, respectively, with each of these aspects. In point of fact, the electron exchange mechanism investigation was in good part responsible for the success of the present studies. For a long time, it was not possible to clarify the relaxation picture, or to get any kind of agreement with theoretical expectations for thermal relaxation processes.³ Then it was shown that a background photon flux arising from the room temperature black body radiation of the waveguide components was incident on the sample.⁴ This infrared radiation photoionized the phosphorus impurities, and the resulting electrons in the conduction band gave rise to the dominant relaxation mechanism at the low temperatures. It was only after this source of relaxation was removed that the thermal relaxation

* Supported in part by the Air Force Office of Scientific Research.

† Now at International Business Machines Research Laboratories, Poughkeepsie, New York.

¹ Spin resonance of group V donors in silicon was first observed by Fletcher, Yager, Pearson, Holden, Read, and Merritt, *Phys. Rev.* **94**, 1392 (1954).

² Preliminary accounts of some aspects of the present work were reported in: (a) A. Honig and E. Stupp, *Phys. Rev. Letters* **1**, 275, (1958); (b) E. Stupp and A. Honig, *Bull. Am. Phys. Soc.* **4**, 261 (1958).

³ Pines, Bardeen, and Slichter, *Phys. Rev.* **106**, 489 (1957).

⁴ A. Honig, *Proceedings of the Kamerlingh-Onnes Memorial Conference on Low-Temperature Physics, Leiden, Holland, 1958* [*Physica* **24**, 1635 (1958)].

processes became accessible to direct measurement and interpretation.

II. ENERGY LEVELS AND EIGENFUNCTIONS OF A PHOSPHORUS ATOM IN A MAGNETIC FIELD

The Hamiltonian representing magnetic interactions for an isolated atom in an external magnetic field \mathbf{H}_0 is given by

$$\mathcal{H} = g_I \mu_0 \mathbf{J} \cdot \mathbf{H}_0 + g_I \mu_0 \mathbf{I} \cdot \mathbf{H}_0 + A \mathbf{I} \cdot \mathbf{J}, \quad (1)$$

where $\hbar \mathbf{I}$, $\hbar \mathbf{J}$ are, respectively, the total angular momenta of the nucleus and electrons; g_I , g_J are, respectively, the nuclear and electronic g factors in terms of the Bohr magneton μ_0 (g positive for a negative magnetic moment according to molecular beam usage), and A is the hyperfine interaction constant.

For an atom whose electronic ground state is $^2S_{1/2}$, as is approximately the case for a phosphorus atom in silicon, the hyperfine interaction constant A is given by the well known Fermi formula

$$A = \frac{16}{3} \pi \mu_0 \frac{\mu_I}{I} |\psi(0)|^2, \quad (2)$$

where $|\psi(0)|^2$ is the probability of finding the s electron at the center of the nucleus.

The energy levels associated with this Hamiltonian are given by the Breit-Rabi formula. In the case of phosphorus, whose nuclear spin $I = \frac{1}{2}$, the energy levels reduce to

W_{m_I, m_J}

$$= \frac{1}{2} A \left\{ -\frac{1}{2} + \frac{2g_I}{g_J - g_I} (m_I + m_J) x + (2m_I m_J + m_J - m_I + \frac{1}{2}) \times [1 + 2(m_I + m_J)x + x^2]^{\frac{1}{2}} \right\}, \quad (3)$$

$x = (g_J - g_I) \mu_0 H_0 / A$. (States labelled with high-field quantum numbers.)

In Fig. 1, Eq. (3) is plotted for the case of a phosphorus atom in silicon. The magnetic moment of phosphorus is positive (g_I negative).

The true eigenstates $\phi(m_I, m_J)$ are linear combinations of the eigenstates $\psi(m_I, m_J)$ of the strong field Hamiltonian, i.e., Eq. (1) without the $A \mathbf{I} \cdot \mathbf{J}$ term. Thus

$$\phi(m_I, m_J) = a_{m_I, m_J} \psi(m_I, m_J) + b_{m_I \pm 1, m_J \mp 1} \psi(m_I \pm 1, m_J \mp 1), \quad (4)$$

where the restriction that different $(m_I + m_J)$ states cannot be mixed follows from the fact that $A \mathbf{I} \cdot \mathbf{J}$ is diagonal in $m_F = (m_I + m_J)$. The a and b coefficients⁵

⁵ See, for example, H. Salwen, Phys. Rev. **101**, 623 (1956). He obtains a and b in the F, m_F representation, from which it is simple to get our Eq. (5).

are given by

$$a_{m_I, m_J} = [1/2(1+x^2)^{\frac{1}{2}}] \{ [(1+x^2)^{\frac{1}{2}} + 1]^{\frac{1}{2}} + [(1+x^2)^{\frac{1}{2}} - 1]^{\frac{1}{2}} \}, \quad (5)$$

$$b_{m_I \pm 1, m_J \mp 1} = [1/2(1+x^2)^{\frac{1}{2}}] \{ [(1+x^2)^{\frac{1}{2}} + 1]^{\frac{1}{2}} - [(1+x^2)^{\frac{1}{2}} - 1]^{\frac{1}{2}} \},$$

where x has the definition given in Eq. (3). The only two states that are mixed in our case are the $(m_I = \frac{1}{2}, m_J = -\frac{1}{2})$ and the $(m_I = -\frac{1}{2}, m_J = \frac{1}{2})$ states.

The Hamiltonian in Eq. (1) is for an isolated phosphorus atom in an external laboratory magnetic field \mathbf{H}_0 . However, the presence of magnetic neighboring atoms and nuclei contributes to the total Hamiltonian. This contribution can be taken into account by adding to the Hamiltonian of the i th phosphorus atom [Eq. (1)] the following terms:

$\mathcal{H}_{\text{neighboring atoms}}$

$$= \mathbf{J}_i \cdot \sum_j A_{ij} (\text{Si}^{29}) \mathbf{I}_j (\text{Si}^{29}) + (g_J \mu_0 \mathbf{J}_i + g_I \mu_0 \mathbf{I}_i) \cdot \sum_j \left\langle \frac{\mathbf{u}_j (\text{Si}^{29})}{r_{ij}^3} - \frac{3\mathbf{r}_{ij} \mathbf{u}_j (\text{Si}^{29}) \cdot \mathbf{r}_{ij}}{r_{ij}^5} \right\rangle_{\text{Av}}$$

$$+ (g_J \mu_0 \mathbf{J}_i + g_I \mu_0 \mathbf{I}_i) \cdot \sum_k \left\langle \frac{\mathbf{u}_k^{\text{el}}}{r_{ik}^3} - \frac{3\mathbf{r}_{ik} \mathbf{u}_k^{\text{el}} \cdot \mathbf{r}_{ik}}{r_{ik}^5} \right\rangle_{\text{Av}}. \quad (6)$$

The first term gives the Fermi s -state interaction of the i th electron with the various Si^{29} nuclei (4.68% natural abundance) contained in the electron's orbit,

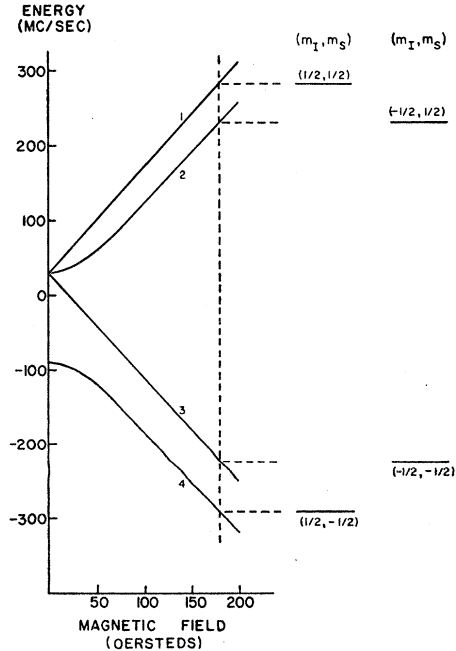


Fig. 1. Magnetic energy levels of a phosphorus impurity atom in silicon as a function of the magnetic field. At the right, a convenient representation for these four levels at a given field value is illustrated.

and the second and third terms give the dipolar interactions with the Si^{29} nuclei and with the other electrons associated with neighboring impurity sites. The averaging in the brackets in the summations is performed over r_{ij} . The inhomogeneous broadening of the resonances and the energy level widths are described by this Hamiltonian.

III. RELAXATION MODES, TIMES, AND PROBABILITIES

If we choose a particular external magnetic field, the four energy levels given in Eq. (3) can be conveniently represented by the arrangement at the right in Fig. 1. The various modes of relaxation possible for this system are shown in Fig. 2. We follow the notation of Pines, Bardeen, and Slichter³ (hereafter referred to as PBS) in designating τ_X and τ_S . In high fields the subscript X stands for "cross relaxation" (simultaneous electron and nuclear spin flips in opposite senses), and the subscript S refers to "direct or vertical relaxation" (electron spin flip only). In weak fields, the significance of the parenthetic description no longer remains; nevertheless, relaxation between the levels at low fields will be denoted with the same subscripts as for the corresponding high-field levels. The τ_N and $\tau_{X'}$ designations are, for the high-field case, associated with a nuclear spin flip only and with simultaneous electron and nuclear spin flips in the same sense, respectively. Again, in low fields, we keep the notation even though the descriptive terminology is no longer meaningful. We will also use the term "horizontal relaxation modes" in referring to τ_X , $\tau_{X'}$, and τ_N (in each, $\Delta m_I = \pm 1$). We summarize the selection rules associated with the various modes of relaxation in terms of high-field quantum numbers:

$$\begin{aligned} \tau_S: \quad \Delta m_S = \pm 1, \quad \Delta m_I = 0, \\ \tau_X: \quad \Delta m_S = \pm 1, \quad \Delta m_I = \mp 1, \\ \tau_N: \quad \Delta m_S = 0, \quad \Delta m_I = \pm 1, \\ \tau_{X'}: \quad \Delta m_S = \pm 1, \quad \Delta m_I = \pm 1. \end{aligned}$$

For certain experiments, it is necessary to make a further distinction for horizontal relaxation modes associated with the Si^{29} hyperfine interaction, but for our present purposes, these may be neglected. It should be noted that there may be several concurrently acting mechanisms for each of the modes of relaxation distinguished above, and that the subscripts do not refer to specific mechanisms but rather to any mechanism(s) with the selection rules denoted above.

The relaxation time τ is the time constant which appears in the expression for the simple exponential approach to Boltzmann equilibrium of the population differences between levels. We wish now to relate the τ 's to relaxation probabilities, which we denote by $2W_S$, $2W_X$, $2W_{X'}$, $2W_N$. Consider two levels, a and b , of energy E_a and E_b . Then for a given spin-lattice coupling mechanism, one can calculate the transition

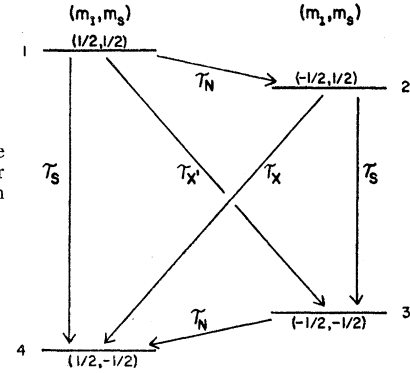


FIG. 2. Spin-lattice relaxation modes for a phosphorus atom in silicon.

probabilities $W_{a \rightarrow b}$ and $W_{b \rightarrow a}$ induced by the lattice. When these transition probabilities arise from interaction with a reservoir which remains always in thermal equilibrium, the relation

$$W_{b \rightarrow a}/W_{a \rightarrow b} = e^{\Delta E/kT} \quad (7)$$

holds, where $\Delta E = E_b - E_a$. It is convenient to define a quantity W as the geometric mean of $W_{b \rightarrow a}$ and $W_{a \rightarrow b}$. Then $W_{b \rightarrow a} = W \exp(\Delta E/2kT)$, and $W_{a \rightarrow b} = W \exp(-\Delta E/2kT)$. In terms of the transition probabilities, the familiar dynamic equations

$$\begin{aligned} \dot{n}_a &= -W_{a \rightarrow b}n_a + W_{b \rightarrow a}n_b \\ &= -W e^{(-\Delta E/2kT)}n_a + W e^{(\Delta E/2kT)}n_b, \\ \dot{n}_b &= W_{a \rightarrow b}n_a - W_{b \rightarrow a}n_b \\ &= W e^{(\Delta E/2kT)}n_a - W e^{(-\Delta E/2kT)}n_b \end{aligned} \quad (8)$$

result, where n_a and n_b represent the populations of levels a and b , respectively. Defining $n = n_a - n_b$, and $N = n_a + n_b$, one readily obtains the equation

$$\dot{n} = 2WN \sinh(\Delta E/2kT) - 2Wn \cosh(\Delta E/2kT), \quad (8a)$$

whose solution is

$$\frac{n(t) - n(\infty)}{n(0) - n(\infty)} = e^{-[2W \cosh(\Delta E/2kT)t]}. \quad (9)$$

The relaxation to equilibrium is seen to be governed by the relaxation time τ , which from Eq. (9) is given by

$$\tau = [2W \cosh(\Delta E/2kT)]^{-1}. \quad (10)$$

The equilibrium value of $n(t)$, denoted by $n(\infty)$, is given by

$$n(\infty) = N \tanh(\Delta E/2kT). \quad (11)$$

τ is the quantity we measure experimentally, whereas the relaxation probability $2W$ is the quantity in terms of which our results are interpreted. We note that if several mechanisms simultaneously contribute to the relaxation between two given levels, the $2W$'s are additive. When more than two levels are involved, a simple exponential does not in general describe the approach to equilibrium. A convenient way to represent the differential equations when many levels are involved is in matrix form.⁶ For example, in phosphorus-doped

⁶ J. W. Culvahouse and F. M. Pipkin, Phys. Rev. **109**, 319 (1958).

silicon, where the levels indicated in Fig. 1 approach equilibrium via the modes listed above, we get:

$$\begin{pmatrix} \dot{n}_1 \\ \dot{n}_2 \\ \dot{n}_3 \\ \dot{n}_4 \end{pmatrix} = \begin{pmatrix} -(W_S\alpha^{\frac{1}{2}} + W_X\alpha^{\frac{1}{2}} + W_N) & W_N & \frac{W_{X'}}{\alpha^{\frac{1}{2}}} & \frac{W_S}{\alpha^{\frac{1}{2}}} \\ W_N & -(W_S\alpha^{\frac{1}{2}} + W_X\alpha^{\frac{1}{2}} + W_N) & \frac{W_S}{\alpha^{\frac{1}{2}}} & \frac{W_X}{\alpha^{\frac{1}{2}}} \\ W_X\alpha^{\frac{1}{2}} & W_S\alpha^{\frac{1}{2}} & -\left(\frac{W_S + W_{X'}}{\alpha^{\frac{1}{2}}} + W_N\right) & W_N \\ W_S\alpha^{\frac{1}{2}} & W_X\alpha^{\frac{1}{2}} & W_N & -\left(\frac{W_S + W_X}{\alpha^{\frac{1}{2}}} + W_N\right) \end{pmatrix} \begin{pmatrix} n_1 \\ n_2 \\ n_3 \\ n_4 \end{pmatrix}, \quad (12)$$

where $\alpha = e^{(E_1 - E_4)/kT} \simeq e^{2\mu_0 H/kT}$, and $(E_1 - E_2)$ and $(E_3 - E_4)$ are taken ~ 0 , which is a good approximation in all of our applications. When the various modes of relaxation are of comparable magnitudes, the solution of Eq. (12) requires the extensive use of a computer. However, when one *mode* is predominant, a near exponential relaxation occurs, and the equations can be solved approximately in a simple manner. In the case of phosphorus-doped silicon, it will be seen that we can separately deduce from the experiments the times associated with the horizontal relaxation modes, and that in all but a few cases, $W_{\text{horiz. modes}} < \frac{1}{5}W_S$. Thus, we can utilize an approximately exponential solution of the relaxation equations to determine W_S without resorting to machine computation, and small corrections due to $W_{\text{horiz. modes}}$ can be added. Also, in determining the constituents of the horizontal modes, quantitative conclusions can be made without machine computation.

IV. EXPERIMENTAL TECHNIQUES FOR MEASURING RELAXATION TIMES

A. Generalities

To observe the resonances of inhomogeneously broadened lines when the spin-lattice and spin-spin relaxation times are long, it is usually convenient to observe adiabatic rapid passage on the dispersion mode. One can in this way obtain large signals at ordinary microwave powers, and a field modulation and narrow band detection scheme can be profitably employed. Under these conditions, the signal amplitude will depend upon experimental parameters such as microwave power, dc magnetic field sweep rate, and modulating magnetic field frequency and amplitude in a fairly complicated manner. However, if these factors are held constant, reproducible signal amplitudes, which are proportional to the population differences between the energy levels under consideration, can be obtained over fairly long time periods (order of hours) to within about 3%. The dispersion mode can be observed either by unbalancing the phase in the bucking arm of a microwave bridge, or by tuning the

klystron to the side of the resonant cavity mode. This latter technique was generally used since better consistency of the signal amplitude could be maintained. A modulation frequency of about 850 cps was used, and the amplitude of the modulating field was kept below 0.5 oersted. The microwave power used was such that the adiabatic condition was approximately satisfied.

B. τ_S Measurements

For the high-field measurements (greater than 1500 oersteds), the method used to measure τ_S was straightforward. The populations of the levels under consideration were equalized by traversing the resonance many times, using high-modulation field amplitude, until the fast passage signal had disappeared. The growth of the population difference was then observed for various values of elapsed time, t . τ_S results immediately from the slope on a semilog plot of $[n(t) - n(\infty)] / [n(0) - n(\infty)]$ vs t , as is evident from Eq. (9). The fact that all resonances are *measured* at 3000 oersteds introduces negligible, or at least a correctable, error because the relaxation time at 3000 oersteds, τ_{3000} , is long compared to the time needed to take a measurement. $n(0)$ and $n(t)$ are of course easily measured, but the equilibrium value of n , $n(\infty)$, which appears in the quantity to be plotted, can be a problem for very long relaxation times such as are encountered in our experiments (sometimes exceeding 10^5 seconds). To be sure, the relaxation time τ can be obtained without direct knowledge of $n(\infty)$, but the accuracy is severely limited, and with an amplitude reproducibility of $\sim 3\%$ of which our equipment is capable, it would be necessary to wait a time of the order of $\tau/2$ to obtain sufficient departure from linear growth in order to measure τ to a precision of about 15%. Naturally, the longer one waits, the better would be the accuracy. On the other hand, if $n(\infty)$ is known, a fair value of the relaxation time for very short elapsed times can be obtained; the limit on how small a time can be used is

imposed principally⁷ by signal to noise considerations. We have measured some of the relaxation times to 10% accuracy in elapsed times of $\sim\tau/10$. To obtain $n(\infty)$, advantage is taken of the relatively short relaxation times encountered at high fields. In all samples, at 10 000 oersteds, $\tau_{10\ 000}$ is less than 7 minutes. Thus $n(\infty)$ at 10 000 oersteds and $\tau_{10\ 000}$ can be measured carefully once. This done, $n(\infty)$ at any field can be calibrated using Eq. (11). As an example of the procedure, suppose one requires the full amplitude $n(\infty)$ at 1000 oersteds which we denote by $n(\infty)_{1000}$. The signal amplitude after a 180 second wait at 10 000 oersteds is first measured. Call this signal $n(180)_{10\ 000}$, where a proportionality factor between signal amplitude and n is understood. (This proportionality factor cancels in the final result.) The full amplitude signal at 10 000 oersteds is given by

$$n(\infty)_{10\ 000} = n(180)_{10\ 000} (1 - e^{-180/\tau_{10\ 000}})^{-1}.$$

Then from Eq. (11), we get

$$n(\infty)_{1000} = n(180)_{10\ 000} (1 - e^{-180/\tau_{10\ 000}})^{-1} \times \frac{\tanh[(\mu/kT) \times 1000]}{\tanh[(\mu/kT) \times 10\ 000]}.$$

The validity of this procedure was checked experimentally.

The low-field τ_S measurements are made in essentially the same way, except that decay of a known amount of magnetization accumulated at high field is measured as a function of time spent at the low fields. In this way, good signal to noise ratios are always

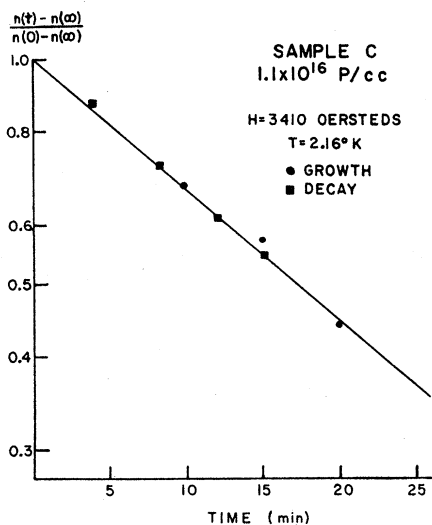


FIG. 3. Semilogarithmic plot illustrating the equivalence of the signal growth and the signal decay techniques for measuring relaxation time.

⁷ In some samples, a few percent of the total number of spins relax faster than the main body of spins, and short time relaxation determinations can lead to large errors in τ .

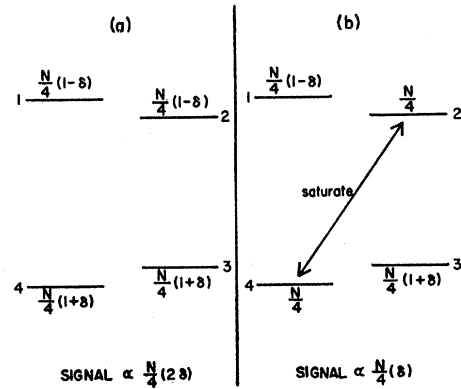


FIG. 4. Determination of the dominant mode of relaxation: (a) If τ_S , after waiting a given time after equalization of all levels, both signals are proportional to 2δ . (b) After waiting same time and then saturating forbidden transition, signal is reduced by a factor of 2. If τ_X were dominant, signal would be zero in (b).

obtained, even at the lowest fields. Between 1500 and 3500 oersteds, the two methods (growth and decay) were checked against each other and agreed well. In Fig. 3, we plot on the same semilog graph the growth and decay functions against time for one of the samples.

In a four level system such as we have here, the procedure just described could yield misleading results if τ_X , rather than τ_S , were the dominant relaxation mechanism. There are several ways to be certain that we are dealing with τ_S and not τ_X . One way is to carry out measurements for times $t \sim \tau$. If $n(\infty)_{H_0}$ is calculated as indicated above, a straight line on a semilog plot will be obtained only if τ_S is dominant. Under a pure τ_X , a straight line would be obtained only if $n(\infty)$ were set equal to one-half the value calculated according to the above prescription. Another method would be to measure τ_X separately (see next paragraph). A third method, and one we have frequently employed, is described in the following. One waits a certain time after saturation to build up a difference of population between the upper and lower states. Then the guide is rotated approximately 45° so that the microwave H field has a component along the direction of the static magnetic field \mathbf{H}_0 and the $(m_I = \frac{1}{2}, m_J = -\frac{1}{2}) \leftrightarrow (m_I = -\frac{1}{2}, m_J = +\frac{1}{2})$ transition is saturated. This is the so-called forbidden transition, for which Jeffries⁸ had demonstrated that a sufficiently large microwave magnetic field along \mathbf{H}_0 could induce transitions. The transitions result because of the admixture of (m_I, m_J) and $(m_I \pm 1, m_J \mp 1)$ states due to hyperfine interaction, as indicated in Eqs. (4) and (5). Subsequent to this saturation of the forbidden transition the guide is rotated back to its normal position and the signal intensities are measured. Figure 4 illustrates the consequences of the above operations when τ_S is the only relaxation mode present. The resonances are seen to be equal in size, and have half the amplitude they would normally have if the

⁸ C. D. Jeffries, Phys. Rev. **106**, 164 (1957).

forbidden transition had not been saturated. It is readily apparent that if τ_X rather than τ_S were the only relaxation mode, the above operations would result in signals of zero amplitude. Intermediate cases (mixed τ_S and τ_X) can also be analyzed in this manner. In the early experiments, double resonance was employed to analyze the relaxation modes, but infrared leakage through the slit in the cavity⁹ caused an additional relaxation mechanism,⁴ and subsequently, the procedure utilizing the forbidden transitions was employed with unslit cavities on all samples.

C. τ_X , $\tau_{X'}$, and τ_N Measurements

The τ_X , $\tau_{X'}$, and τ_N are treated together in this section because the experiments of necessity involve combinations of these modes. Two methods were used to determine these horizontal relaxation ($\Delta m_I = \pm 1$, $\Delta m_S = 0, \pm 1, \mp 1$) modes. Each method yields a characteristic time and a steady state population situation which depend differently on τ_X , $\tau_{X'}$, and τ_N . Thus, the two methods complement each other, and enable one to obtain information on the relative importances of τ_X , $\tau_{X'}$, and τ_N .

The first method utilizes the Overhauser effect applied to discrete hyperfine lines. It has previously been employed by Pipkin^{6,10} and Feher¹¹ to measure τ_X . A brief description of our version follows. Levels $1 \leftrightarrow 4$ and $2 \leftrightarrow 3$ (see Fig. 1) are saturated quasi-continuously by sweeping through both lines at a rate such that the sweep period is short compared to both τ_X and τ_S . For the moment, let us assume τ_X is the only horizontal relaxation mode present. At $t=0$, $n_1=n_2=n_3=n_4=N/4$. At $t=\infty$, $n_4/n_2 = \exp[(E_2 - E_4)/kT]$, where this difference in population is brought about by the τ_X relaxation mode. The approach to equilibrium is exponential with a characteristic time ($2\tau_X$).¹² Observation of $(n_4 - n_2)$ is made by turning off the saturating power for the vertical levels, rotating the guide and saturating levels $2 \leftrightarrow 4$, and finally rotating the guide back to its normal position and measuring the resonance signals. The signals are equal in magnitude, and both are inverted. Each signal is proportional to $\frac{1}{2}(n_4 - n_2)$, and τ_X is obtained from the formula $(n_4 - n_2) = (N/2) \tanh(\mu H/kT)(1 - e^{-t/2\tau_X})$. The method differs from that used by Feher in that he used double resonance rather than the "forbidden transition" to make $(n_4 - n_2)$ observable. The experimental limitation of the method is that the τ_X determination is restricted to the magnetic field value corresponding to resonance, which is determined by the operating frequency of the spectrometer. This is so because of the

requirement of keeping levels $1 \leftrightarrow 4$ and $2 \leftrightarrow 3$ saturated.¹³ Also, to use the method, τ_S must be at least of the order of a minute so that the populations do not change much while saturating the forbidden transitions. The double resonance method is somewhat faster in this respect, but still requires a τ_S of at least 10 seconds.

So far, we have illustrated the method when τ_X is assumed to be the only horizontal relaxation mode of importance. If we now introduce $\tau_{X'}$ and τ_N , we find that Eq. (12) governs the dynamics of the relaxation provided $W_S/\alpha^{\frac{1}{2}}$ and $W_S\alpha^{\frac{1}{2}}$ which appear in that equation are replaced by \mathfrak{W}_{rf} , where \mathfrak{W}_{rf} is the transition rate produced by the saturating microwave field. If $\mathfrak{W}_{rf} \gg W_X$, $W_{X'}$, and W_N , Eq. (12) has the simple solution

$$\frac{(n_4 - n_2)(t) - (n_4 - n_2)(\infty)}{(n_4 - n_2)(0) - (n_4 - n_2)(\infty)} = e^{-[(W_X + W_{X'}) \cosh(\mu H/kT) + 2W_N]t}, \quad (13)$$

where

$$(n_4 - n_2)(\infty) = \frac{N}{2} \frac{(W_X - W_{X'}) \sinh(\mu H/kT)}{(W_X + W_{X'}) \cosh(\mu H/kT) + 2W_N}. \quad (14)$$

In the usual experimental application, $(n_4 - n_2)(0) = 0$, and

$$(n_4 - n_2)(t) = \frac{N}{2} \frac{(W_X - W_{X'}) \sinh(\mu H/kT)}{(W_X + W_{X'}) \cosh(\mu H/kT) + 2W_N} \times (1 - e^{-[(W_X + W_{X'}) \cosh(\mu H/kT) + 2W_N]t}). \quad (15)$$

Thus, from Eq. (15), it is seen that if one could wait long enough and determine $(n_4 - n_2)(\infty)$, all the W 's could be separated out. As it happens, at 1.25°K this is not feasible since the times involved are of the order of days. On the other hand, if one waits times *short* compared to $[(W_X + W_{X'}) \cosh(\mu H/kT) + 2W_N]^{-1}$ and if $\cosh(\mu H/kT) \simeq 1$ as is approximately the case for our Overhauser data, then

$$(n_4 - n_2)(t) \simeq (N/2) \sinh(\mu H/kT)(W_X - W_{X'})t \times [1 - (W_X + W_{X'} + 2W_N)(t/2)]. \quad (16)$$

Since the values of W_X , $W_{X'}$, and W_N are mostly unknown, the easiest way to interpret the experimental results is to express Eq. (16) in the form

$$(n_4 - n_2)(t) \simeq (N/2) \sinh(\mu H/kT)(1 - e^{-2Wt}), \quad (17)$$

where " $2W$ " is the *apparent relaxation probability* deduced when no account is taken of the reduced steady state population difference exhibited in Eq. (15). It is still understood that t is short compared to

¹³ It is possible, when τ_S is very long, to maintain the quasi-continuous saturation at fields other than the resonance field, by field cycling techniques.

⁹ The slit in the cavity is required to permit the radio-frequency magnetic field to penetrate to the sample.

¹⁰ Francis M. Pipkin, Phys. Rev. **112**, 935 (1958).

¹¹ G. Feher, *Proceedings of the Kamerlingh-Onnes Memorial Conference on Low-Temperature Physics, Leiden, Holland, 1958* [Physica **24**, 805 (1958)].

¹² The characteristic time is $2\tau_X$, rather than τ_X , because the number of spins transferred via τ_X has to be shared between the vertical levels.

$[(W_X + W_{X'}) \cosh(\mu H/kT) + 2W_N]^{-1}$. From (16) and (17),

$$\begin{aligned} "2W"(Overhauser) &\simeq "1/\tau"(Overhauser) \\ &\simeq (W_X - W_{X'})[1 - (W_{X'} + W_N)t], \quad (18) \end{aligned}$$

and $(W_X - W_{X'})$ can be obtained directly from the experiments when t is small. An indication of the magnitude of $(W_{X'} + W_N)$ can also be obtained when the measurements are of sufficient accuracy. It should be mentioned here that care must be exercised in saturating the vertical transitions in order to assure a sufficiently small accompanying transition rate for the forbidden transition. Otherwise, inducing the forbidden transition contributes the same effect as a W_N . The microwave H field used to saturate the vertical transitions should be just large enough to maintain the near equality of the populations of the vertical levels and the waveguide should be carefully oriented so as to minimize the component of the microwave H field in the direction of the static field \mathbf{H}_0 . Taking these precautions, we estimate that an artificial τ_N of this type of about 500 hours is still present at 1.25°K. If it were shorter than this by a factor of 10, it would have been necessary to take considerable trouble to avoid completely the forbidden transition.

The second method for determining horizontal relaxation modes consists simply of polarizing the nuclei into a given m_I state,¹⁴ and then waiting at various values of the magnetic field and temperature. The depolarization due to the τ_X , $\tau_{X'}$, and τ_N relaxation is obtained by measuring the ratio of the amplitudes of the two resonance lines. This method has the advantage that for sufficiently long horizontal relaxation times (order of at least several minutes at 3000 oersteds), the relaxation times can be measured throughout the entire magnetic field range using a single frequency spectrometer, since all measurements are made at 3000 oersteds. The waiting and attendant depolarizing can, of course, occur at any magnetic field.

The analysis of this situation is again simple provided $W_S > W_X$, $W_{X'}$ and W_N . The quantity of interest is $[(n_2 + n_3) - (n_1 + n_4)](t)$, for which the following expression is derived:

$$\begin{aligned} &\frac{[(n_2 + n_3) - (n_1 + n_4)](t)}{[(n_2 + n_3) - (n_1 + n_4)](0)} \\ &= \exp \left\{ - \left[\frac{W_X + W_{X'}}{\cosh(\mu H/kT)} + 2W_N \right] t \right\}. \quad (19) \end{aligned}$$

Thus, the experimentally observed quantity

$$\frac{[(n_2 + n_3) - (n_1 + n_4)](t)}{[(n_2 + n_3) - (n_1 + n_4)](0)}$$

¹⁴ The method of polarization is that of Jeffries (see reference 8). In Sec. IVB of this paper, the description of the technique used for determining the dominant relaxation mode is identical to the polarizing technique. Nuclear polarization exceeding 30% is easily obtained by two successive applications of the method at 1.25°K and 10 000 oersteds.

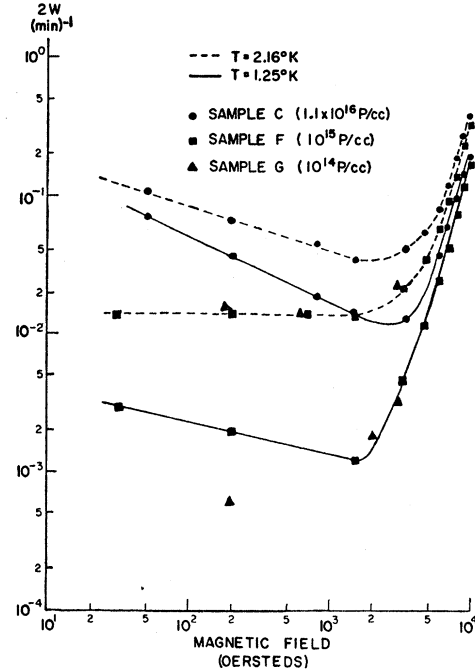


FIG. 5. Logarithmic plot of the relaxation probability $2W$ as a function of magnetic field for a few samples.

decays exponentially to zero with a characteristic time

$$\tau(\text{decay}) = \left[\frac{W_X + W_{X'}}{\cosh \mu H/kT} + 2W_N \right]^{-1}. \quad (20)$$

From Eqs. (18) and (20), it can be seen that at moderate magnetic fields where $\cosh \mu H/kT \sim 1$, the horizontal relaxation associated with decay always appears faster than the horizontal relaxation associated with the Overhauser method. The difference between them is $\sim 2(W_{X'} + W_N)$.

The method of decay can also be extended to high temperatures where the Boltzmann factor is small. For a horizontal relaxation time measurement at 4.2°K, the nuclei were polarized at 1.25°K, and then the helium bath was quickly raised to 4.2° by means of a heating coil placed at the bottom of the helium bath. The depolarization at 4.2° was observed by monitoring the ratio of the amplitudes of the two resonances as in the lower temperature measurements.

V. EXPERIMENTAL RESULTS

In Figs. 5 and 6, the magnetic field and temperature dependences of the relaxation probability are plotted on a log-log scale, for several samples. For most of the points, $W_X < \frac{1}{5}W_S$, and the growth or decay is closely exponential in time. For those few points where this is not true, the $2W$ are calculated as if a simple exponential governed the relaxation, using experimental relaxing times much shorter than τ . From inspection of the data, three distinct mechanisms are immediately

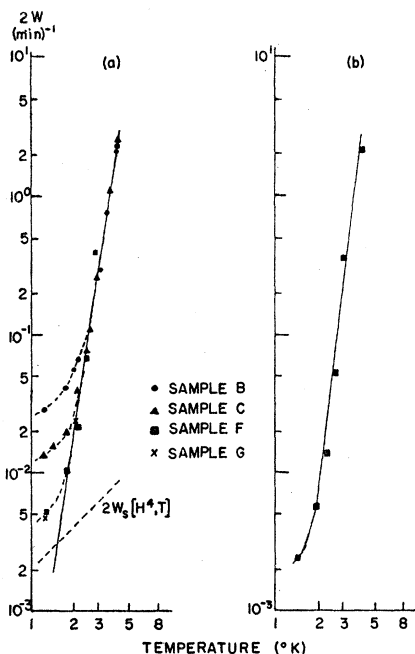


FIG. 6. (a) Logarithmic plot of the relaxation probability $2W$ as a function of temperature. The magnetic field is 3400 oersteds. (b) Same plot for sample F after subtracting $2W_s(\text{conc.})$, $2W_s(H^4, T)$ and contributions from the horizontal modes.

evident, since one of the three clearly dominates in a unique field-temperature region. At high-magnetic fields, and at temperatures below about 2.5°K , we see a concentration independent mechanism whose relaxation probability goes as H^4 , and approximately as T (Fig. 5). The small deviations for samples of different concentrations are due to the small contribution of a concentration dependent mechanism which persists even at strong magnetic fields. At temperatures above about 2.5°K for the more concentrated samples, and throughout almost the entire temperature range for the dilute samples, we see another concentration independent mechanism (Fig. 6) whose principal identifying feature is that the relaxation probability depends very strongly on temperature.¹⁵ The actual dependence is slightly greater than the seventh power of temperature, but we will refer to this mechanism as the T^7 mechanism. For this mechanism, no field dependence is evident within experimental error, as can be seen from the 2.16°K curve of the low concentration samples (Fig. 5). The third mechanism dominates at low-magnetic fields and low temperatures (Fig. 5). Its principal feature is concentration dependence, and it is also characterized by a relaxation probability which depends approximately on H^{-3} and T . In addition to these three obviously discernible mechanisms, the horizontal relaxation modes make a contribution to the resultant (experimental) relaxation probability. These are of

¹⁵ G. Feher and E. A. Gere, Bull. Am. Phys. Soc. 3, 415 (1958), have independently reported on this mechanism.

small magnitude throughout the temperature and magnetic field range, i.e., they never dominate the relaxation picture. Since they can be determined separately, as was discussed in Sec. IVC, their contribution to the resultant relaxation probability can be taken into account. Indeed when these four mechanisms and modes are added together, they account for almost all the experimental points. However, in the region between 2000 and 3000 oersteds for the dilute samples at 1.25°K , a fifth mechanism is required. The $1/\tau$ associated with it is very long, about $2 \times 10^{-5} \text{ sec}^{-1}$. It is not possible to determine this mechanism's properties accurately since the errors associated with it are large. Nevertheless, it appears to be field independent over a limited range (or at most have an H^1 dependence). Temperature dependence was not determined because the T^7 mechanism so rapidly dominates as the temperature is raised above 1.25°K .¹⁶ There is some evidence which suggests that this mechanism may be associated with minority impurity concentration. An infrared photon leak⁴ was ruled out as the cause of this small relaxation effect.

We now examine more detailed features of each of the mechanisms. We first consider the temperature dependence of the H^4 mechanism. Measurements of relaxation taken at a high magnetic field value where the H^4 mechanism dominates are selected. The small contributions to the relaxation made by the concentration dependent mechanism and T^7 mechanism are extrapolated to the high field and subtracted from the measured relaxation probability. (The horizontal modes produce less than a 1% effect and can be neglected here.) This leaves the relaxation probability associated solely with the H^4 mechanism, which we denote by $2W_s(H^4, T)$. It is well known that in a single phonon process, $W_{\text{emission}} \propto e^{2\mu H/kT} (e^{2\mu H/kT} - 1)^{-1}$ and $W_{\text{absorption}} \propto (e^{2\mu H/kT} - 1)^{-1}$. Thus, from our definition of W given in Sec. II, $W \propto e^{\mu H/kT} (e^{2\mu H/kT} - 1)^{-1}$. In Fig. 7, $2W_s(H^4, T) \times \cosh(\mu H/kT) (= 1/\tau_s)$ is plotted against $e^{\mu H/kT} (e^{2\mu H/kT} - 1)^{-1} \times \cosh \mu H/kT (= \coth \mu H/kT)$. The reason for the factor $\cosh \mu H/kT$ in the abscissa and ordinate is that W_s , being a geometric mean between the emission and absorption probabilities, vanishes at 0°K , whereas $2W_s \cosh(\mu H/kT)$, or $1/\tau_s$, does not vanish, and thus, we are able to illustrate the relaxation induced by the zero point vibrations in the type plot we have chosen. It is seen that a straight line is obtained, whose intercept at 0°K is a positive value. The value of the intercept should be numerically equal to the slope if the first order phonon process indeed describes the temperature dependence, and this is seen to be the case.

Varying the orientation of the samples with respect to the magnetic field direction produced no change outside of the experimental error (about 5%) in the

¹⁶ At temperatures below 1.25°K , we should be able to obtain the temperature dependence of this mechanism. A liquid He^3 cooled paramagnetic resonance apparatus which is presently under construction will make this possible in the future.

TABLE I. List of samples used in this investigation and their type of crystal growth.

Sample	Room temp resistivity	Concentration of uncompensated phosphorus atoms ^a	Crystal growth	Remarks
A	0.27 ohm-cm	$3.5 \times 10^{16}/\text{cc}$	Czochralski	DuPont silicon starting material (about 100 ohm-cm <i>p</i> -type)
B	0.47 ohm-cm	$1.7 \times 10^{16}/\text{cc}$	Czochralski	DuPont silicon starting material (about 100 ohm-cm <i>p</i> -type)
C	0.65 ohm-cm	$1.1 \times 10^{16}/\text{cc}$	Czochralski	DuPont silicon starting material (about 100 ohm-cm <i>p</i> -type)
D	1.4 ohm-cm	$4.2 \times 10^{15}/\text{cc}$	Floating zone	High resistivity (about 1500 ohm-cm) Merck silicon starting material
E	4.1 ohm-cm	$1.3 \times 10^{15}/\text{cc}$	Floating zone	DuPont silicon starting material One premelt before crystal growth
F	5.5 ohm-cm	$1.0 \times 10^{15}/\text{cc}$	Floating zone	High resistivity (about 1500 ohm-cm) Merck silicon starting material
G	45-55 ohm-cm	$\sim 1 \times 10^{14}/\text{cc}$	Floating zone	High resistivity (about 1500 ohm-cm) Merck silicon starting material

^a See reference 19.

relaxation probability associated with the H^4 mechanism. Thus we conclude that the H^4 first order phonon relaxation mechanism is isotropic within the limits stated.

The T^7 mechanism, which is concentration independent and field independent, suggests a Raman, i.e., two phonon, type process. From the curve of Fig. 6(a), it is clear that the Raman relaxation dominates at 3000 oersteds for the dilute samples down to about 2.0°K. When the H^4 mechanism and horizontal modes are subtracted off for one of the dilute samples, as in Fig. 6(b), the T^7 Raman mechanism can be followed throughout the temperature range. The exponent of the temperature is 7.5 ± 0.3 near 4.2°K, and about 7 at 2.0°K. At 1.25°K, the deviation from the T^7 curve is due to the "fifth mechanism" described above. The field dependence, or rather independence, of the Raman mechanism is seen in Fig. 5 for the dilute samples, and has been demonstrated at higher temperatures for more concentrated samples. The Raman relaxation mechanism has been found to be independent of sample orientation within the experimental error.

The concentration dependent mechanism was seen in Fig. 5 to be predominant at high concentrations, low temperature, and low magnetic field. We denote the relaxation probability associated solely with the concentration dependent mechanism by $2W_S(\text{conc.})$. $2W_S(\text{conc.})$ is equal to the observed relaxation probability minus the sum of the $2W$'s connected with the H^4 and T^7 mechanisms, and the horizontal modes. In Fig. 8, $2W_S(\text{conc.})$ is plotted against concentration of neutral donors. The concentration of neutral (uncompensated) phosphorus donors was obtained from four types of information: room temperature resistivity, signal strength in the paramagnetic resonance spectrometer, resonance amplitude associated with the exchange line,¹⁷ and spin-spin relaxation rate.¹⁸ Good agreement of *relative* concentrations was obtained

¹⁷ Charles P. Slichter, Phys. Rev. **99**, 479 (1955).

¹⁸ A. Honig and E. Stupp, Bull. Am. Phys. Soc. **3**, 9 (1958). The concentration dependence has since been investigated.

among the methods. The actual concentrations were obtained from the resistivities, using the curve given by Prince.¹⁹ In Table I, we list some of the properties of the samples we have used. Returning now to Fig. 8, for concentrations above about 10^{16} P/cc, we see the onset of the rapid increase of $2W_S(\text{conc.})$ with concentration.²⁰ Below 10^{16} P/cc, $2W_S(\text{conc.})$ falls off approximately linearly with concentration, sample E providing an exception. Sample E, however, was grown from about 100 ohm-cm Dupont silicon (Table I) and was premelted in a crucible. It is therefore quite likely to have a high-percentage compensation. It is this sample which leads us to suspect that minority impurity concentration is responsible for a separate relaxation mechanism. A relaxation measurement on sample E at 3000 oersteds supports this contention. The field dependence for this mechanism in sample E is very much like that encountered with the "fifth mechanism" on the less compensated dilute samples. Since the

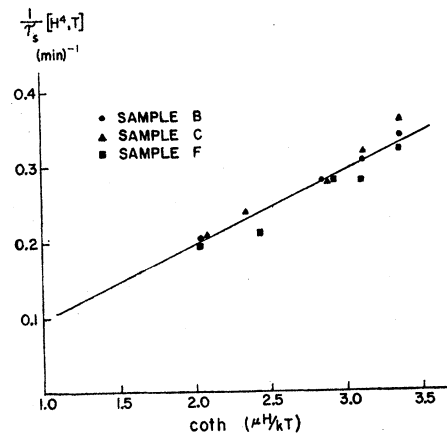


FIG. 7. Single phonon process temperature dependence: Reciprocal relaxation time of the H^4 mechanism $[=2W_S(H^4, T) \times \cosh \mu H / kT]$ plotted against $\coth(\mu H / kT) \{ = \exp(\mu H / kT) \times [\exp(2\mu H / kT) - 1]^{-1} \times \cosh(\mu H / kT) \}$.

¹⁹ M. B. Prince, Phys. Rev. **93**, 1204 (1954).

²⁰ Feher, Fletcher, and Gere, Phys. Rev. **100**, 1784 (1955).

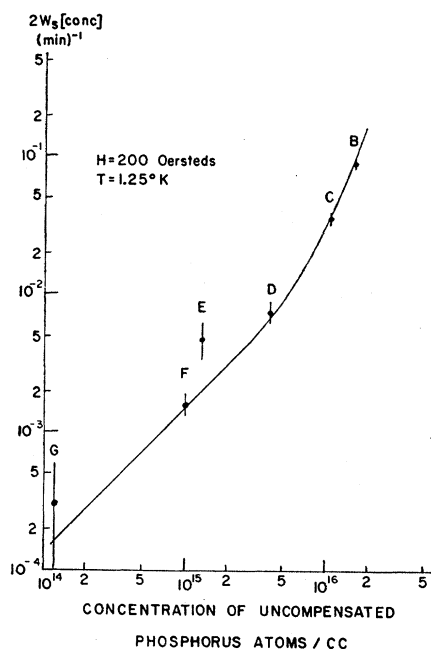


FIG. 8. Logarithmic plot of the concentration dependence of $2W_S(\text{conc.})$ at 200 oersteds.

dilute samples come from similar starting material (Table I), an interpretation of the fifth mechanism as associated with minority impurity concentration is not inconsistent with our data.

Figure 9 gives the temperature dependence of the concentration dependent relaxation probability for several samples at two values of the magnetic field. The relaxation probability depends nearly linearly on T , which suggests that a first order phonon process may be involved. In Fig. 10, we plot relaxation probability *vs* energy difference between levels rather than against magnetic field, and note that the parameter upon which the relaxation probability depends is not the value of the external magnetic field but rather the energy level separation. This is seen most strikingly at the low values of magnetic field, where, for a given value of the magnetic field, the energy differences between levels corresponding to the low field ($1 \leftrightarrow 4$) and high field ($2 \leftrightarrow 3$) resonance lines differ considerably, and as a consequence, the low-field and high-field lines relax at different rates. (In Fig. 5, to avoid confusion, the average relaxation rate of the high- and low-field lines was plotted against the magnetic field.) The relaxation probability was found to be isotropic for this mechanism.

The $\tau_{\text{horiz. modes}}$ data are summarized in Table II. We recall from Eq. (18) that the time of measurement enters into the interpretation of “ τ ” (Overhauser). Hence, the waiting time t for the measurement is also given in the table for the Overhauser measurements. It should be stressed at this point that both “ τ ” (Overhauser) and τ (decay) are not themselves the hori-

zontal relaxation times, but are just characteristic times for particular experimental procedures. Even in the simple case where $W_{X'}$ and W_N are both zero, the conventional cross relaxation time $\tau_X (\simeq \frac{1}{2} W_X)$ would be given by $\frac{1}{2}$ “ τ ” (Overhauser) and by $\sim \frac{1}{2} \tau$ (decay), from Eqs. (18) and (20). The physical reason for the one-half factor is given in footnote 12.

The errors associated with these measurements are large due to the long times involved, the signal to noise ratio, and some small nuclear polarization effects probably associated with close pairs. Nevertheless, significant conclusions can be extracted from the data.

1. The close agreement at 2.15°K between “ τ ” (Overhauser) and τ (decay) indicates that W_X is considerably greater than $W_{X'}$ or W_N . Using the results of Sec. IVC, we can state that at 2.16°K, $0 \leq W_{X'} < \sim 0.2W_X$, $0 \leq W_N < \sim 0.1W_X$. If $W_{X'}$ and W_N were equal to zero, $\tau_X (\simeq \frac{1}{2} W_X)$ would be equal to 3.0 ± 0.4 hours.

2. At 4.2°K, where we have only a τ (decay) measurement, it is not immediately evident that W_X is the dominant mode. However, it would be very surprising if $W_{X'}$ had a different temperature dependence from W_X , since $W_{X'}$ presumably arises from modulation of an *anisotropic* hyperfine interaction,¹⁰ and W_X from modulation of the closely related isotropic hyperfine interaction. Since $W_{X'}$ is much less than W_X at 2.16°K, we therefore expect this will also be true at 4.2°K. As for W_N , if we use the result that it is less than

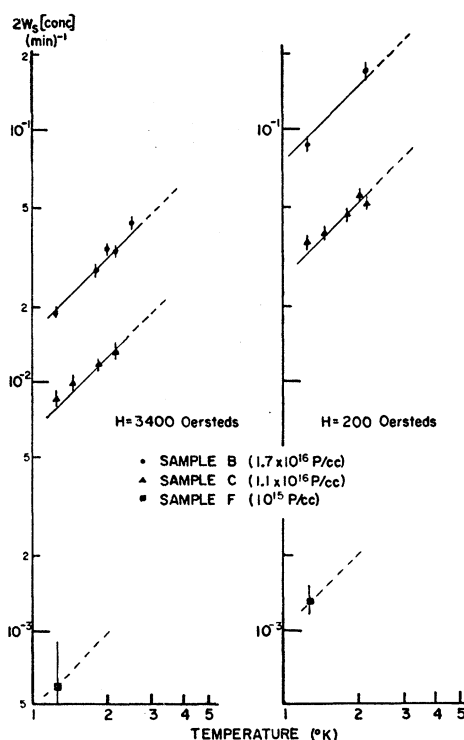


FIG. 9. Temperature dependence of the concentration dependent mechanism, plotted logarithmically.

TABLE II. Horizontal relaxation time τ (decay) at various values of temperature and magnetic field. In one of the 3400 oersteds columns, " τ " (Overhauser) is given; t is the elapsed time for the measurement.

Sample	Temp.	H_0 (oersteds)						
		10 800	9800	3400	3400 (Overhauser)	1000	200	55
B (1.7×10^{16})	1.25°K							10±4 min
C (1.1×10^{16})	2.16°K							
	1.25°K		26 $_{-5}^{+6}$ hr	32 $_{-4}^{+6}$ hr	5.7±1.3 hr ($t=3$ hr)			
	2.16°K		5±1.5 hr	4.4±1 hr	38 $_{-6}^{+10}$ hr ($t=5$ hr)	30 $_{-7}^{+10}$ hr	10.5 $_{-2}^{+4}$ hr	29±6 min
F (1×10^{15})	4.2°K			5.4±1.4 min	6.0±0.8 hr ($t=5$ hr)			
	1.25°K	17±8 hr	22 $_{-6}^{+8}$ hr	32 $_{-6}^{+10}$ hr	40 $_{-10}^{+20}$ hr ($t=5$ hr)			16.5±5 hr
	2.16°K		4.0 $_{-0.6}^{+2}$	4.8 $_{-1.2}^{+1.6}$ hr	6.6±1.6 hr ($t=3$ hr)			
	4.2°K			4.2±1.4 min				

$W_X/10$ at 2.16°K, it would require at least a tenth power dependence on temperature to dominate at 4.2°K. This is highly unlikely. Thus it seems reasonable to assume that at 4.2°K, W_X dominates. In this case, $T^{6.5}$ (the exponent is $6.5_{-0.6}^{+0.8}$) gives the temperature dependence of W_X between 4.2°K and 2.16°K. This temperature dependence suggests a Raman process. The magnetic field independence at 2.16°K lends further support.

3. At 1.25°K, the " τ " (Overhauser) and τ (decay) on samples C and F at 3000 oersteds indicate that W_X is considerably greater than $W_{X'}$ or W_N , since τ (decay) is not very different from " τ " (Overhauser). Using the analysis in Sec. IVC, we can say that $0 \leq W_{X'} < \sim 0.2W_X$, and $0 \leq W_N < \sim 0.2W_X$. It also follows that τ_X exceeds ~ 16 hours, $\tau_{X'}$ is greater than ~ 80 hours, and τ_N exceeds ~ 80 hours.

4. The rest of the 1.25° data at the various magnetic fields does not support a quadratic magnetic field dependence of the relaxation probability, as is predicted

by PBS³ for a first order phonon τ_X mechanism. Our high field results appear incompatible with a τ_X of ~ 5 hours at 1.2°K and 8000 oersteds, reported by Feher and Gere.¹⁵

5. At the low fields (200 oersteds and below), a definitely concentration dependent mechanism enters into τ (decay). The explanation of this mechanism is given in the next section.

VI. THEORETICAL MECHANISMS

The discussion in this section deals with a few of the mechanisms we have observed experimentally. We attempt to identify the theoretical origin of some of the mechanisms by comparing temperature, field, and concentration dependence and order of magnitude of the relaxation probability predicted by theory, with the experimental results. Exact calculations will not be made.

The first relaxation mechanism about which we inquire is the first order phonon mechanism with the H^4 dependence. PBS³ have made a calculation based on spin-orbit coupling, and employing the deformation potential method. They find that two terms contribute to the relaxation probability:

$$\begin{aligned} (a) & \quad (\psi_{0-}, E_{1+} \Delta \psi_{0+}), \\ (b) & \quad (E_{0+} - E_{0-}) (\psi_{0-}, \delta \psi_{+}), \end{aligned} \quad (21)$$

where ψ_{0+} and ψ_{0-} are the wave functions for a spin up and spin down electron, respectively, and $E_{1+} \Delta$ and $\delta \psi_{+}$ are the change in total energy and wave function for a spin up electron, due to a dilation Δ . Term (a) in Eq. (21) yields the relaxation probability given by PBS

$$2W = \frac{E_{1+}^2 \omega_0^4 kT}{2\pi \hbar^2 \rho s^7} [(\Delta g)_{\text{imp.}}^2 \langle r_{n0} \rangle^2 + (\Delta g)_{\text{Si}}^2 9a_0^2], \quad (22)$$

where $\Delta g_{\text{imp.}}$ is the shift from the free electron g value associated with the impurity center, and Δg_{Si} is the shift in g associated with the silicon atoms. a_0 is the Bohr radius, and r_{n0} is the dipole matrix element for a transition from an n th excited state to the ground state. Actually, a high-temperature approximation was given in (22). The exact expression for $2W$ at low

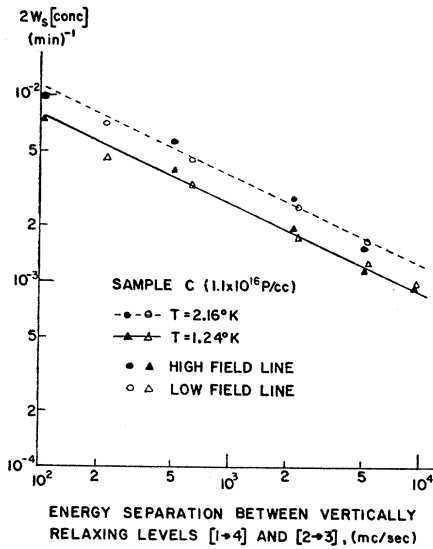


FIG. 10. Logarithmic plot of the dependence of $2W_S$ (conc.) on the energy separation between states 1 and 4 (low-field line) and 2 and 3 (high-field line). Pairs of points originate at the same magnetic field. For example, the low-field point at 222 Mc/sec and the high-field point at 104 Mc/sec both were obtained at 50 oersteds.

temperature is:

$$2W = \frac{E_{1+}^2}{2\pi\hbar^2\rho s^7} [(\Delta g)_{\text{imp.}}^2 \langle r_{n0} \rangle^2 + (\Delta g)_{\text{SI}}^2 9a_0^2] \omega_0^5 \times e^{\hbar\omega_0/2kT} (e^{\hbar\omega_0/kT} - 1)^{-1}. \quad (23)$$

This is seen to have close to an H_0^4 (or ω_0^4) and T dependence.²¹ However, when allowance is made for "Van Vleck cancellation,"²² as was pointed out by Abrahams,²³ another H^2 dependence enters. Thus, the first term has an H^6 dependence, and its order of magnitude at a field of 3000 oersteds and 1°K is about 10^9 seconds. Even at the highest fields we have explored (11 000 oersteds), it is still three orders of magnitude longer than the experimental times we have observed. It is conceivable that at fields of several hundred thousand oersteds, this mechanism could become observable.

Term (b) in (21) arises from the modulation of the admixture of higher states in the wave function, due to the lattice distortions. This term has an H^2 and T dependence, but on correcting for "Van Vleck cancellation," an extra H^2 factor appears, thus giving this term a field dependence in agreement with experiment. The order of magnitude estimate made by PBS consists of determining the relaxation time for unbound conduction electrons and multiplying by a factor representing the ratio of bound to unbound matrix element. This latter reducing factor arises because the bound electron responds approximately adiabatically to the variations in potential caused by the lattice vibrations. Subsequent reduction factors due to density of states and to Van Vleck cancellation yield the figure of 10^8 seconds quoted by Abrahams.²³ However, it may be that the PBS estimate of the reduction factor in relaxation probability due to adiabaticity is too large. PBS used $\hbar\omega_0/ev$ for the estimate, but since the electron is bound only with energies of the order of a few hundredths of ev , the reduction factor may have been overestimated by about three orders of magnitude, since the factor enters a matrix element and gets squared. This mechanism could thus lead to an estimation of relaxation time at 3000 oersteds and 1.2°K of about 3×10^6 seconds. The observed time is 3.9×10^4 seconds. While one order of magnitude discrepancy still remains, the nature of the estimate is such as to prevent discounting this term as the origin of the first order phonon process.

A Raman process has been calculated by Abrahams,²³ who obtains a T^{13} dependence of relaxation probability on temperature, and approximate field independence. His result disagrees with experiment with regard to order of magnitude and temperature dependence. Abrahams calculated a second order perturbation

process linear in the deformation. There are, of course, several other types of calculation that lead to a two phonon Raman process. For example, the two phonons can be introduced via first order perturbation theory through terms quadratic in the deformation. This type of calculation has been considered in previous theoretical studies of Raman relaxation processes.²⁴ In these calculations, at low temperatures, there frequently results a T^7 temperature dependence and magnetic field independence. The field independence comes about from neglect of the spin energy in comparison with the energies of the effective phonons involved in the relaxation. For nuclear spin relaxation, this approximation is excellent. For electronic spin relaxation, however, at very low temperatures, it is of interest to estimate the amount of field dependence to be expected when the spin energy is not neglected. An integral of the form

$$I = \int_0^{\theta_D/T} \frac{\zeta^3(\zeta + \zeta_0)^3 e^{\zeta} d\zeta}{(e^{\zeta + \zeta_0} - 1)(e^{\zeta} - 1)}, \quad (24)$$

where $\zeta = \hbar\omega/kT$, $\zeta_0 = \hbar\omega_0/kT$, and θ_D = Debye temperature, always appears in a Raman process having a T^7 dependence. By assuming $\theta_D/T = \infty$, which is a very good approximation for silicon in the liquid helium temperature region, the following expression is obtained:

$$I = e^{-\zeta_0} \left(\Gamma(7) \sum_{j=0, i \leq j}^{j=\infty} \frac{e^{-\zeta_0(j-i)}}{(j+i)^7} + 3\Gamma(6)\zeta_0 \sum_{j=0, i \leq j}^{j=\infty} \frac{e^{-\zeta_0(j-i)}}{(j+i)^6} + 3\Gamma(5)\zeta_0^2 \sum_{j=0, i \leq j}^{j=\infty} \frac{e^{-\zeta_0(j-i)}}{(j+i)^5} + \Gamma(4)\zeta_0^3 \sum_{j=0, i \leq j}^{j=\infty} \frac{e^{-\zeta_0(j-i)}}{(j+i)^4} \right). \quad (25)$$

This yields at 1.25°K a decrease of W with increasing magnetic field of less than 0.1% between 0 and 3000 oersteds, and of about 2.2% between 3000 and 10 000 oersteds. The experimental data in the region where the Raman process is dominant are not of sufficient accuracy to test this slight field dependence. Besides, slight magnetic field dependence is also expected to arise because of the change of excited state wave functions with magnetic field.

The concentration dependent mechanism is one for which no theory previously suggested appears to be applicable. It is an unusual relaxation process, in the sense that it can be dominant for concentrations of less than $10^{15}/\text{cc}$, and also because the relaxation probability increases with decreasing magnetic field. A possible theoretical mechanism will be outlined here.

The essential idea is that relaxation of the main body of spins is brought about by spin diffusion from rapidly

²¹ Between 3000 and 10 000 gauss, at 1.25°K, the exact formula yields an $H_0^{3.95}$ dependence. The exact H and T dependences were used in the experimental analysis.

²² J. H. Van Vleck, Phys. Rev. **57**, 426 (1940).

²³ E. Abrahams, Phys. Rev. **107**, 491 (1957).

²⁴ For the first such calculation, see I. Waller, Z. Physik **79**, 370 (1932).

relaxing centers. These centers are composed of close pairs of impurities, which are present by virtue of the random distribution of impurities. The pairs can consist of *ionized phosphorus-neutral phosphorus* or *neutral phosphorus-neutral phosphorus*. It is the latter which we believe produce what has been called the $2W_S(\text{conc.})$ mechanism, and the immediate discussion will be concerned primarily with them. The electrons associated with close pairs have wave functions different from those of isolated phosphorus atoms, because the electrons are in large orbits which encompass both phosphorus nuclei. Thus, the wave function of a close pair is governed by the Coulomb interaction with *two* phosphorus nuclei, and by an electron exchange interaction denoted by $J\mathbf{S}_1 \cdot \mathbf{S}_2$, where J is the exchange energy constant and is a function of the separation between pairs. (For an *ion-neutral* pair, the exchange interaction is naturally absent.) PBS³ calculated the relaxation time associated with modulation of J by the lattice vibrations, and obtained very long times. Even by choosing very close pairs,²⁵ it does not seem possible to get sufficiently short times from this mechanism. However, due to the nonspherically symmetric Coulomb potential and also to electron correlation effects, we expect a modified spin-orbit coupling to cause a very rapid relaxation of the electrons associated with a close pair. If this is so, then distributed essentially randomly in space are a given concentration of "relaxation centers." From these centers, we assert the main body of electron spins associated with isolated phosphorus atoms relax via a spin diffusion process. We may note that this mechanism is very similar in principle to one proposed by Bloembergen to account for nuclear spin relaxation in ionic crystals.²⁶

Let us now consider in more detail the behavior of this mechanism and inquire as to its validity by comparing some predictions of the theory with experiment. We consider *neutral-neutral* pairs and assume for illustrative purposes only that those pairs which are separated by between 15 and 20 angstrom units make up the effective relaxation centers. We wish to find the concentration of these pairs as a function of total phosphorus concentration. For a random distribution of atoms, the distribution law of the nearest neighbor is given by²⁷

$$w(r) = \exp[-4\pi r^3 n/3] 4\pi r^2 n, \quad (26)$$

where $w(r)dr$ gives the probability that a neighbor to a given atom is between r and $r+dr$, and n is the average number of atoms per unit volume. From Eq. (26), it is readily seen that the relative concentration of pairs separated by 15 to 20 angstroms increases linearly with

total phosphorus concentration, up to total phosphorus concentrations of about 10^{18} P/cc. Thus, if the bottleneck to the whole sample relaxation is the relaxation rate of the pair centers themselves and not the diffusion rate, we should expect a relaxation probability going directly as the concentration. This was experimentally observed in a limited region. We next consider the magnetic field dependence. If the spin to lattice relaxation of the close pair centers is the bottleneck to the whole sample relaxation, then the linear dependence on temperature would indicate a single phonon process. This would mean that $2W_S(\text{conc.})$ should go as H^2 or H^4 , and not as the observed H^{-3} . Hence, to explain the field dependence there must be a process in the total relaxation picture which becomes more efficient with decreasing H_0 . One possibility for such a process is the spin coupling of the close pair center to the first neighboring phosphorus atom. If the g factor associated with an effective pair is changed a few parts in a thousand by the modified spin-orbit coupling characteristic of a close pair, then at high fields the spin energy of the pair center will deviate from the spin energy of an isolated phosphorus atom by amounts comparable to the inhomogeneous line width, thus impeding energy exchange between the relaxation center and the isolated atom. At the low fields, the energy difference due to the g factor deviation becomes less, while the inhomogeneous line width remains the same. Spin energy exchange between relaxation center and isolated atom should thus occur more freely at the low-magnetic fields. With a bottleneck such as this, it is not clear how the linear temperature dependence arises. It would seem as if the spin energy exchange between the pair and an isolated atom should be *linked* to the spin-lattice relaxation of the pair center, rather than merely *sequential* to it.

The fact that sample *E* (Fig. 8) exhibits an extra relaxation mechanism, plus the fact that this sample is suspected of having a large percentage compensation compared to the other samples, leads us to consider compensation dependent mechanisms. One such mechanism related to the above discussion involves ion-neutral pairs as relaxation centers. The question arises why the ion-neutral pair relaxation does not exhibit the same field dependence attributed to the neutral-neutral pair. A possible answer is that the effective ion-neutral pairs are very close neighbors which could have smaller g factor deviations than do more distantly separated pairs. (For neutral-neutral pairs, it was seen²⁵ that these very close neighbors are ineffective relaxation centers because the triplet state is not populated.) Further experimental work and theoretical work on the two nuclei centers (solid state "hydrogen molecules and molecule ions") is clearly in order to test the validity of these last speculations.

The order of magnitude of the relaxation time of the centers needed to provide agreement with experiment would be about 1 second or less, if 15–20 angstrom spacing actually corresponded to the relevant centers.

²⁵ For very close pairs, due to the Pauli exclusion principle, probably only the lower lying singlet electron spin state is appreciably occupied. This state cannot contribute to the relaxation process.

²⁶ N. Bloembergen, *Physica* **15**, 386 (1949).

²⁷ See, e.g., S. Chandrasekhar, *Revs. Modern Phys.* **15**, 1 (1943).

This pair relaxation time does not seem at all unreasonable. With the 10^{16} P/cc sample, a few percent of the spins exhibit the exchange resonance.^{1,17} Of these few percent, most have a rapid passage line shape indicating long relaxation time, but a detectable fraction show a line shape corresponding to quite short relaxation times (much less than a second).

We now consider the second part of the relaxation process, namely the diffusion of spin. If we start out with the level populations equal (resonances saturated), the electron spins are at a high temperature. The relaxation centers (pairs), rapidly equilibrating with the cold lattice, act as heat sinks, and are the agency whereby the rest of the spins get cooled via a diffusion process. This is the hypothesis for the $2W_S(\text{conc.})$ mechanism. Conversely, we can start with the spins all cooled to the lattice temperature, and then heat up a given fraction of the spins. This can be done if thermal equilibrium of the spin system with the lattice is established and then a small part of the magnetic spectrum of the inhomogeneously broadened line is saturated. The electrons being resonated act as a *heat source* for the rest of the spins, just as in the relaxation case the pair centers acted as *heat sinks*. Since the electrons at a given value of the magnetic spectrum are randomly spacially separated, just as the pair centers are randomly spacially separated, the situations are quite parallel, and the diffusion rate can be investigated in this reverse way. We found the time needed for diffusion to be a function of sample concentration, but independent of temperature in the region investigated, 1.25°K to 2.16°K. For 10^{16} P/cc, roughly a minute and a half was required for the resonance signal to be diminished to one half its initial value when about 1% of the total number of spins at the center of the resonance envelope was continually saturated. For the 4×10^{15} sample, this time was about 5 minutes, and for the 10^{15} P/cc sample, about 50 minutes were required. These times are consistent with the hypothesis that diffusion is not the bottleneck in the relaxation. If the microwave power was not continually on, very much less diffusion took place. A principal argument raised against spin diffusion processes for inhomogeneously broadened resonances is that energy is not conserved in a macroscopic diffusion. *Momentarily* "burning a hole" in a resonance line and then waiting is exactly a situation where no energy can enter the spin system, and energy changes have to come from the dipolar energy of the spin system.²⁸ Since the hyperfine width is large compared to

the dipolar width in our case, macroscopic diffusion of spin energy is forbidden, as is observed. However, when the microwave power remains on, a source of energy is continually present. Consider a slightly non-monochromatic microwave energy source. A given spin can absorb a microwave photon in one local field and emit a photon in a different local field, because of the change of the electron's own local field between absorption and emission, brought about by spin diffusion. In this way, if the microwave power is constantly on, net energy can be transferred continually in small bits, the microwave source steadily returning to the dipolar system the energy lent by the dipolar system to neighboring packets for microscopic spin diffusion. In this way, it appears possible for macroscopic spin diffusion to occur. The situation for the relaxation centers is parallel, in that the phonon source is non-monochromatic and is continually on.²⁹

To summarize: the concentration dependence of $2W_S(\text{conc.})$ as well as independent diffusion experiments are in agreement with the theory we propose for the concentration dependent mechanism. The understanding of the field and temperature dependence requires further theoretical analysis. It is possible that the mechanism outlined here also contributes to the very rapid rise of relaxation probability with concentrations above 10^{16} P/cc. For example, if clusters of three phosphorus atoms form efficient relaxation centers, and diffusion is fast enough to spread the relaxation, clusters of three could contribute a mechanism whose relaxation probability goes as the square of the concentration.

For the τ_X mechanisms, the only theoretical calculations that have been made are those of PBS.³ They considered a first order phonon process in which the hyperfine interaction was modulated by the lattice vibrations. An H^2 and T dependence of the relaxation probability was predicted. Our results in the region where a first order process could be important (1.25°K) do not yield a quadratic field dependence. At present, we do not understand the dominant mechanism at 1.25°K. The Raman process which dominates above 2.0°K perhaps may be accounted for by a simple extension of the PBS interaction to terms quadratic in the deformation Δ .

The low field increase of $W_{\text{horiz. modes}}$ is actually a manifestation of the concentration dependent τ_S mechanism. What we normally refer to as a τ_S mechanism at high fields is a mechanism with matrix elements connecting states (m_I, m_S) and $(m_I, m_S \pm 1)$. At low fields, because levels (m_I, m_S) and $(m_I \pm 1, m_S \mp 1)$ are mixed, as can be seen from Eq. (4), the same matrix elements produce τ_N transitions. The relation of W_N to

²⁸ We are not considering here the case discussed by G. Feher and E. A. Gere, Phys. Rev. **114**, 1245 (1959) where the Si^{29} system is also presumed to change its energy. Our functional dependence of diffusion on microwave power is not consistent with either a $\tau_X(\text{Si}^{29})$ process, or the inducing of forbidden transitions via an anisotropic Si^{29} hyperfine coupling, though this latter possibility requires further investigation. The cross relaxation scheme of Bloembergen *et al.* seems too slow to account for the observed diffusion in our case, and ought not to depend on the microwave power.

²⁹ If the anisotropic Si^{29} hyperfine coupling is responsible for the observed "spin diffusion" with the microwaves on, we would also expect diffusion from *relaxation centers* to take place.

W_S should be given simply by

$$W_N = |b_{m_I \pm 1, m_J \mp 1}|^2 W_S, \quad (27)$$

where $|b_{m_I \pm 1, m_J \mp 1}|^2$ is given as a function of magnetic field in Eq. (5). Since $W_S(\text{conc.})$ depends on the energy difference between relaxing levels (see Fig. 10), it is different for the two possible W_N transitions, and the average $\langle W_S \rangle_{av}$ should be used. In Table III, the $2W_N$ calculated according to Eq. (27), and the experimental values of the horizontal relaxation probability $2W$ (decay), are listed. The 200 oersteds result is fairly close to the calculated value of $2W_N$. The 55 and 75 oersteds experimental results are somewhat larger than the $2W_N$ predicted by theory. Moreover, at 55 and 75 oersteds, there is clear evidence for a concentration dependent W_X mechanism, in addition to the W_N mechanism. This evidence consists of the observation that in the process of nuclear depolarization at the low fields, a population difference builds up between both pairs of vertical levels (1-4 and 2-3) in excess of that associated with the Boltzmann factor at the respective low fields. The explanation of this concentration dependent W_X mechanism is similar to that given for the W_N mechanism above. The W_S mechanism has matrix elements connecting not only (m_I, m_S) and $(m_I, m_S \pm 1)$, but also (m_I, m_S) and (m_I, m_S) . At high fields, these latter $\Delta m_I = 0, \Delta m_S = 0$ transitions have very little effect, but at low fields, because of the appreciable admixture of states, they give rise to W_X relaxation of the observed magnitude. As the magnetic field increases, the W_N is favored over the W_X because the energy level separation involved in the W_X transition increases faster than the energy level separations in the W_N transitions. A small contribution to $W_{\text{horiz. modes}}$ at 55 oersteds can also come from an energy conserving three body spin-spin process in which two phosphorus atoms flip from state 1 to 2, and one phosphorus atom flips from state 4 to 3 (see Fig. 1). Taking into account these last three processes accounts fairly well for the low-field horizontal relaxation data.

VII. CONCLUSION

From a thorough analysis of the spin-lattice relaxation in phosphorus-doped silicon, various magnetic moment-phonon interactions have been identified. Both single phonon and two phonon (Raman) processes

TABLE III. Comparison of low field horizontal relaxation probability $2W$ (decay) with calculated value of $2W_N$.

Sample	Magnetic field	$2\langle W_S \rangle_{av}$ (min^{-1})	$2W_N$ (min^{-1}) calculated	$2W$ (decay) (min^{-1}) experimental
<i>B</i> (1.7×10^{16} P/cc)	55 oersteds	0.34	3.5×10^{-2}	$(1.0 \pm 0.4) \times 10^{-1}$
<i>B</i>	75 oersteds	0.33	2.1×10^{-2}	$(3.5 \pm 0.5) \times 10^{-2}$
<i>C</i> (1.1×10^{16} P/cc)	55 oersteds	0.10	1.1×10^{-2}	$(3.5 \pm 0.7) \times 10^{-2}$
<i>C</i>	75 oersteds	0.10	6.4×10^{-3}	$(1.1 \pm 0.2) \times 10^{-2}$
<i>C</i>	200 oersteds	0.10	1.1×10^{-3}	$(1.6 \pm 0.5) \times 10^{-3}$
<i>F</i> (1×10^{16} P/cc)	55 oersteds	0.0025	2.6×10^{-4}	$(1.0 \pm 0.3) \times 10^{-3}$

were found to be important in the liquid helium temperature region. A concentration dependent mechanism, believed to be associated with close pairs, gives information on the properties of closely spaced impurity sites.

The relaxation measurements provide a means of determining impurity concentration in silicon without recourse to transport phenomena. It might also be remarked that the T^7 temperature dependence may make it possible to use the system as an accurate thermometer in the liquid helium temperature range. The H^4 relaxation mechanism may limit the application of this system as a microwave frequency multiplying maser device.

It should be highly desirable to investigate the more complicated (due to possible quadrupole effects) cases of antimony and arsenic-doped silicon throughout the magnetic field and temperature region as was done here.

VIII. ACKNOWLEDGMENTS

We wish to thank Dr. R. O. Carlson, Dr. D. C. Jillson, and Mr. A. S. Rugare of General Electric Research Laboratories at Schenectady and Syracuse for having kindly provided the silicon samples used in this investigation.

Note added in proof.—In view of the recent theoretical work of Hasegawa (to be published) and Roth [Bull. Am. Phys. Soc. Ser. II, 5, 60 (1960)], in which a first order phonon mechanism was calculated which yields an anisotropic relaxation probability, we reexamined the angular dependence of the H^4 relaxation probability, orienting the [100] and [111] directions along the external magnetic field to bring out the maximum anisotropy. An anisotropic contribution equal to about 50% of the isotropic contribution was indeed found, giving a value for the anisotropic relaxation probability with [111] parallel to the external field of $1.1 \times 10^{-5} \text{ sec}^{-1}$ at 3000 oe and 1.25°K. The H^4 mechanism relaxation probabilities given in this paper are close to the sum of the isotropic probability plus one-half the anisotropic probability, on account of the essentially random orientations generally used.